

ECOLOGY

Hydraulic traits are coordinated with maximum plant height at the global scale

Hui Liu¹, Sean M. Gleason², Guangyou Hao³, Lei Hua^{1,4}, Pengcheng He^{1,4}, Guillermo Goldstein^{5,6}, Qing Ye^{1*}

Water must be transported long distances in tall plants, resulting in increasing hydraulic resistance, which may place limitations on the maximum plant height (H_{\max}) in a given habitat. However, the coordination of hydraulic traits with H_{\max} and habitat aridity remains poorly understood. To explore whether H_{\max} modifies the trade-off between hydraulic efficiency and safety or how water availability might influence the relationship between H_{\max} and other hydraulic traits, we compiled a dataset including H_{\max} and 11 hydraulic traits for 1281 woody species from 369 sites worldwide. We found that taller species from wet habitats exhibited greater xylem efficiency and lower hydraulic safety, wider conduits, lower conduit density, and lower sapwood density, which were all associated with habitat water availability. Plant height and hydraulic functioning appear to represent a single, coordinated axis of variation, aligned primarily with water availability, thus suggesting an important role for this axis in species sorting processes.

INTRODUCTION

Plant height is a straightforward but important trait for plant ecological strategies (1, 2). Height is a crucial component of water balance (3), carbohydrate transport (4), and light interception and may also correlate with leaf economic traits (5). Height is a meaningful predictor of species- and ecosystem-level traits, such as plant volume and aboveground woody biomass (6), and has also been used as an integrative indicator of species richness and environmental stress (7). Furthermore, greater height facilitates access to high-radiation habitats but, as a consequence, results in a longer path length (greater resistance) and greater gravitational potential (8). The classic hypothesis of hydraulic limitation resulting from tree height has long been considered and widely tested (9), which arises from the assumption that, with increasing height, the total path length resistance increases proportionately, making water transport to upper leaves more difficult in large-stature species (3, 10). To avoid embolism resulting from more negative water potential, leaves higher in the canopy are expected to exhibit stronger stomatal control to reduce water loss, but with the consequence of reducing transpiration, photosynthesis, and growth (3, 8, 11).

Beyond the physiological and structural limitations placed on plant height (12), environmental factors are also crucial determinants of plant height across species and biomes. At broad spatial scales, water availability, especially precipitation and potential evapotranspiration (PET), has been emphasized and evaluated as the most important factor that affects plant height. For example, among 22 environmental variables, precipitation in the wettest month was found to be the best factor explaining global patterns of H_{\max} across nearly 6000 species

from 222 field sites (13). Another study reported that annual precipitation was the main predictor of conifer height across the United States (14). An investigation of tall tree species found that their occurrence depended critically on a narrow range of temperature seasonality, as well as high precipitation and high humidity (15). Therefore, both atmospheric and soil aridity represent limitations to attaining tall stature in forest communities. Exploring the global relationships between H_{\max} and hydraulic traits across species could reveal potential linkages between plant height and water transport traits and therefore help us understand the impact of climate change on the distribution of vascular species across the world's terrestrial biomes (16).

Across aridity gradients, species should develop corresponding adaptive strategies to water availability through hydraulic regulation, which must be coordinated with plant height. Specifically, we might expect the maximum efficiency of xylem tissue (hereafter “efficiency”) to be higher in species from wet habitats. Conversely, we might expect arid habitats to favor xylem traits conferring resistance to embolization (hereafter “safety”). Furthermore, if the evolution of high safety and efficiency in the same species is either not possible or represents a substantial loss of performance, then we might expect a safety-efficiency trade-off to arise across species. Several lines of evidence support the idea of a safety-efficiency trade-off within and across species. For example, increasing climatic aridity was associated with a decline in xylem efficiency (sapwood-specific hydraulic conductivity, K_s) and an increase in xylem safety (xylem tension causing 50% loss of maximum conductivity, P50) of European beech (17). Similarly, a weak trade-off was found between K_s and P50 across 424 woody species sampled across a wide range of precipitation, such that species from wet habitats exhibited less negative P50 and higher K_s than species from arid habitats (18). The hydraulic safety margin (the difference between minimum xylem water potential and P50) has been suggested as a meaningful predictor of global aridity tolerance and growth across species (19) and has been found to be relatively convergent across species and biomes (20), which also suggests that fast growth may require highly efficient xylem but at the expense of xylem safety. Considering that greater height should result in more negative leaf water potentials, all else remaining equal, we might therefore expect taller species to exhibit greater safety (more negative P50) and lower K_s . However, this may not be the case because many of the plant traits affecting water balance also change across

Copyright © 2019
The Authors, some
rights reserved;
exclusive licensee
American Association
for the Advancement
of Science. No claim to
original U.S. Government
Works. Distributed
under a Creative
Commons Attribution
NonCommercial
License 4.0 (CC BY-NC).

¹Key Laboratory of Vegetation Restoration and Management of Degraded Ecosystems, Guangdong Provincial Key Laboratory of Applied Botany, South China Botanical Garden, Chinese Academy of Sciences, Xingke Road 723, Tianhe District, Guangzhou 510650, China. ²Water Management and Systems Research Unit, USDA-ARS, Fort Collins, CO 80526, USA. ³Key Laboratory of Forest Ecology and Management, Institute of Applied Ecology, Chinese Academy of Sciences, Shenyang 110010, China. ⁴University of Chinese Academy of Sciences, Yuquan Road 19A, Beijing 100049, China. ⁵Department of Biology, University of Miami, PO Box 249118, Coral Gables, FL 33124, USA. ⁶Departamento de Ecología, Genética y Evolución, Facultad de Ciencias Exactas y Naturales, Universidad de Buenos Aires, Ciudad Universitaria, Núñez, Buenos Aires C1428EGA, Argentina.

*Corresponding author. Email: qye@scbg.ac.cn

habitats. Therefore, a more integrative approach (21) is required to understand the consequences of plant height on hydraulic coordination across species and habitats.

The Whitehead-Edwards-Jarvis proportionality (21) (hereafter “Darcy’s law”) represents an integration of climate and plant attributes influencing water transport through xylem tissue and can be rearranged and expressed as

$$K_s \propto \frac{Ht \cdot g_s \cdot \frac{A_L}{A_S} \cdot D}{(\Psi_S - \Psi_L)} \quad (1)$$

where K_s is the sapwood-specific hydraulic conductivity, Ht is the tree height, g_s is the stomatal conductance, A_L/A_S is the evaporative surface area of leaves relative to the sapwood cross sectional area, D is the leaf-to-atmosphere vapor pressure deficit, and $(\Psi_S - \Psi_L)$ is the pressure potential difference between soil and leaf. Considering that K_s varies considerably more than any other trait in Darcy’s law across species and habitats (22), it is possible that K_s evolved to compensate for both increasing height and increasing hydraulic demand that should be expected to arise from greater leaf-to-sapwood area ratio (A_L/A_S) (23, 24). If this is true, then K_s may serve to maintain rates of gas exchange across species differing in height and A_L/A_S and thus facilitate water balance (21, 22).

It is important to realize that K_s cannot compensate for increasing height in all habitats. The scaling of vessel diameter is relatively convergent across species, and this leads to wider vessels at the base of tall plants than short plants (25, 26), and wide conduits are more susceptible to freeze-thaw embolization than are narrow conduits (27). Furthermore, the effect of K_s on whole-plant conductance may be dampened by increasing sapwood capacitance in tall plants, which serves to release water to the transpiration stream during periods of high evaporative demand and low soil water potential (28, 29). If this effect of sapwood capacitance is meaningful, then it may also confound a trade-off between P50 and K_s in humid habitats, such that we may not expect increasing K_s to be necessarily associated with a more vulnerable xylem (30).

In this study, we examined the strength and direction of the linkage between xylem anatomy and physiology with maximum plant height at the global scale. Given that woody species tend to grow taller in regions with higher water availability, we aimed to answer the following questions: (1) Is the hydraulic safety-efficiency trade-off across species underpinned by the close alignment of hydraulic traits and plant height? (2) Does greater xylem efficiency across species compensate for longer path length resistance (height) and wider leaf-to-sapwood area ratio via Darcy’s law? (3) Do taller species also exhibit wider conduits, lower conduit density, and less dense xylem? (4) Is the observed coordination between height and hydraulic traits also associated with a shift in habitat water availability? Considering that differences in phylogeny, plant structure, and phenology might either drive or confound relationships among plant traits and height, we also addressed each of these questions separately for angiosperms and gymnosperms, for each biome, for trees and shrubs, and for deciduous and evergreen species.

RESULTS

Our study sites covered seven biome types and a marked range of water availability (table S1). Aridity index (AI; please see the abbreviation

glossary in Table 1) values ranged over 50-fold from 0.08 to 4.51 (mean \pm SD is 0.90 ± 0.53), representing arid deserts to tropical rain forests (Fig. 1, A and B). As expected, the maximum plant height (H_{\max}) of each site showed significant positive correlation with AI (Fig. 1C and tables S2 and S3). Across both angiosperms and gymnosperms, H_{\max} increased linearly with actual measured plant height (H_{act}) but did not follow the 1:1 line, indicating that H_{act} tended to be less than H_{\max} throughout its range (fig. S1). Specifically, the $H_{\max} \sim H_{\text{act}}$ slope was steeper across gymnosperms than across angiosperms, such that the H_{act} of gymnosperms was typically less than one-third of H_{\max} , whereas the H_{act} of angiosperms was typically less than one-half of H_{\max} . Hence, it is possible that the poor representation of tall gymnosperm species might have contributed to weak relationships between H_{act} and AI or hydraulic traits for this clade (insets in Figs. 1 and 2 and figs. S2 and S3).

Question 1: Plant height is positively correlated with K_s and P50

H_{\max} increased with increasing K_s across species, with a common standardized major axis (SMA) regression slope among angiosperms and gymnosperms (Fig. 2A and tables S2 and S3). Among biomes, SMA slopes for $H_{\max} \sim K_s$ within angiosperms were all significantly positive except for species from boreal forest (BOR; but $n = 8$) and were significantly shallower for species from tropical seasonal forest (TRS) and tropical rainforest (TRR) than other biomes. Within gymnosperms, only temperate seasonal forest (TMS) species showed a significant positive relationship (table S4). SMA slopes did not differ between shrubs and trees nor between deciduous and evergreen species (tables S5 and S6).

Less negative P50 (lower safety) was associated with larger H_{\max} across species, and the $H_{\max} \sim P50$ SMA slope was steeper for gymnosperms than for angiosperms (Fig. 2B and tables S2 and S3). SMAs revealed significant positive correlations for $H_{\max} \sim P50$ among biomes, with TMS angiosperms exhibiting the steepest slope. In contrast, all biomes exhibited a common slope within gymnosperms (table S4). SMAs for $H_{\max} \sim P50$ were significant for trees, but not for shrubs, within both angiosperms and gymnosperms (table S5). Deciduous and evergreen species exhibited common $H_{\max} \sim P50$ slopes within both angiosperms and gymnosperms (table S6).

A trade-off between K_s and P50 was found, with a steeper SMA regression slope for gymnosperms than for angiosperms (Fig. 2C and tables S2 and S3). SMAs showed significant positive correlations for $K_s \sim P50$ within biomes except that no correlation was evident for TRR angiosperms (table S4). Neither different leaf forms nor life forms exhibited different SMA slopes for angiosperms, whereas within gymnosperms, meaningful comparisons based on life forms and leaf forms could not be made, owing to small sample sizes of shrubs ($n = 10$) and deciduous species ($n = 8$) (tables S5 and S6). When H_{\max} was included as an additional predictor (i.e., $K_s \sim P50 \times H_{\max}$), the best fit linear mixed-effects model (LMM) for angiosperms explained a total of 83% of the variation in K_s ; however, only 9% was contributed by P50 and H_{\max} . Among the random factors, species and site explained 42 and 39%, respectively, of the random variation in K_s . In the linear model (LM) with no random factors, P50 and H_{\max} together explained 13% of the total variation in K_s (Table 2).

Question 2: Darcy’s law

H_{\max} was positively correlated with A_L/A_S but only significant within angiosperms (Fig. 2D and table S3). K_s was positively correlated with $H_{\max} \times A_L/A_S$ and $H_{\text{act}} \times A_L/A_S$, across both angiosperms and

Table 1. Abbreviations for different traits (units), biomes, and method names in this study.

Abbreviation	Index	Unit
Traits		
AI	Aridity index	—
H_{\max}	Maximum plant height	m
H_{act}	Actual measured plant height	m
P50	The xylem tension at 50% loss of the maximum hydraulic conductivity	MPa
K_s	Sapwood-specific hydraulic conductivity	$\text{kg m}^{-1} \text{s}^{-1} \text{MPa}^{-1}$
K_L	Leaf-specific hydraulic conductivity	$\times 10^{-4} \text{kg m}^{-1} \text{s}^{-1} \text{MPa}^{-1}$
Ψ_{pre}	Minimum water potential at predawn	MPa
Ψ_{mid}	Minimum water potential at midday	MPa
Ψ_{tlp}	Leaf turgor loss point	MPa
A_L/A_S	Leaf-to-sapwood area ratio	$\text{m}^2 \text{cm}^{-2}$
WD	Sapwood density	g cm^{-3}
Vdia	Mean tangential vessel diameter for angiosperms or tangential tracheid diameter for gymnosperms	μm
VD	Number of vessels (angiosperms) or tracheids (gymnosperms) per square millimeter	mm^{-2}
VL_{\max}	Maximum vessel length for angiosperms	μm
Eq. 1		
Ht	Tree height	m
g_s	Stomatal conductance	$\text{mol m}^{-2} \text{s}^{-1}$
D	Leaf-to-atmosphere vapor pressure deficit	MPa
$\Psi_S - \Psi_L$	The pressure potential difference between soil and leaf	MPa
Biomes		
DES	Deserts	—
WDS	Woodland/shrubland	—
BOR	Boreal forest	—
TMS	Temperate seasonal forest	—
TMR	Temperate rainforest	—
TRS	Tropical seasonal forest	—
TRR	Tropical rainforest	—
Methods		
SMA	Standardized major axis	—
LMM	Linear mixed-effects model	—
LM	Linear model	—
PCA	Principal components analysis	—
PC	Principal component	—

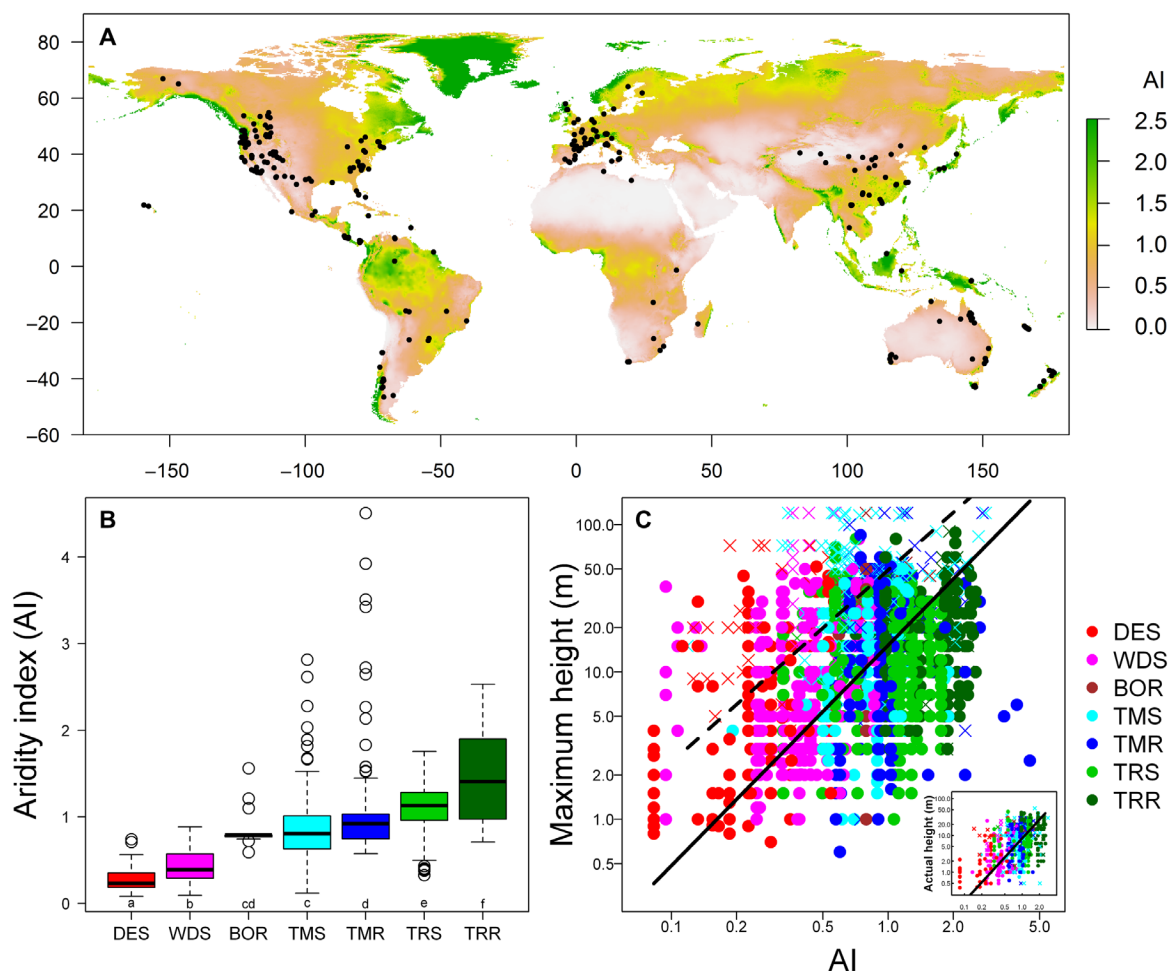


Fig. 1. Study site, AI, and their relationship with plant height. (A) Distribution of the study sites ($n = 369$) relative to the global variation in AI. (B) AI values of the seven biomes in this study. (C) Maximum plant height (inset: actual measured plant height) increased with AI values across biomes. Ranges of AI have been adjusted (A) to show a distinguishable color gradient at the global scale (i.e., AI has a maximum value of 14, and 1.1, 1.6, and 2.2 are the 75th, 90th, and 95th percentiles, respectively). Boxes denote median values and the 25th to 75th percentiles; horizontal lines outside of boxes represent the 10th and 90th percentiles; circles denote outliers; letters under each box represent multiple comparisons (B). Abbreviations for biomes are given in Table 1. In (C), only significant SMA regressions for angiosperms (circles, solid line) and gymnosperms (crosses, dashed line) are shown.

gymnosperms, but the log-log slopes were all significantly less than one (0.69 across angiosperms and 0.75 across gymnosperms; $P < 0.001$ in all cases), thus indicating less than proportional (i.e., non-compensating) scaling (Fig. 2E). For angiosperms, temperate rainforest (TMR) species exhibited the steepest $H_{\max} \sim A_1/A_5$ slopes across biomes, while $H_{\max} \sim A_1/A_5$ slopes did not differ between life forms nor leaf forms (tables S4 to S6).

Question 3: Coordination between plant height and other hydraulic traits

Wider conduit diameter (V_{dia}), lower conduit density (VD), and lower sapwood density (WD) in terminal branches were associated with larger H_{\max} across species. Although SMA slopes for $H_{\max} \sim V_{dia}$ and $H_{\max} \sim VD$ differed significantly between angiosperms and gymnosperms, the slope for $H_{\max} \sim WD$ did not differ between the two clades (Fig. 2, F to H, and tables S2 and S3). $H_{\max} \sim V_{dia}$ and VD showed shallower slopes for angiosperm species from TRS and TRR, but all biomes exhibited a common slope for $H_{\max} \sim WD$ (table S4). Angiosperm shrubs exhibited significantly steeper $H_{\max} \sim V_{dia}$, VD , and WD slopes

than did angiosperm trees. Evergreen angiosperms exhibited a steeper $H_{\max} \sim WD$ slope than did deciduous angiosperms (tables S5 and S6).

For other hydraulic traits, increasing height was associated with less negative minimum water potential at predawn (Ψ_{pre}) and at midday (Ψ_{mid}), with a common SMA slope among angiosperms and gymnosperms (fig. S2). H_{\max} also exhibited significant positive correlations with leaf-specific hydraulic conductivity (K_L) and turgor loss point (Ψ_{tlp}) (fig. S3). Maximum vessel length (only angiosperms, VL_{\max}) showed no pattern with H_{\max} either among biomes or between life forms and leaf forms (tables S3 to S6). Details on comparisons among biomes, between life forms and leaf forms, and LMM and LM results for these traits are reported in appendix S1.

Question 4: Effects of habitat water availability on the coordination between height and hydraulic traits

When AI was involved as a fixed factor (e.g., $H_{\max} \sim \text{trait} \times \text{AI}$), the best fit LMMs for angiosperms explained a total of over 90% variation in H_{\max} (91 to 99% for the six hydraulic traits in Table 2A), but within which only 4 to 33% was contributed by fixed factors (hydraulic trait

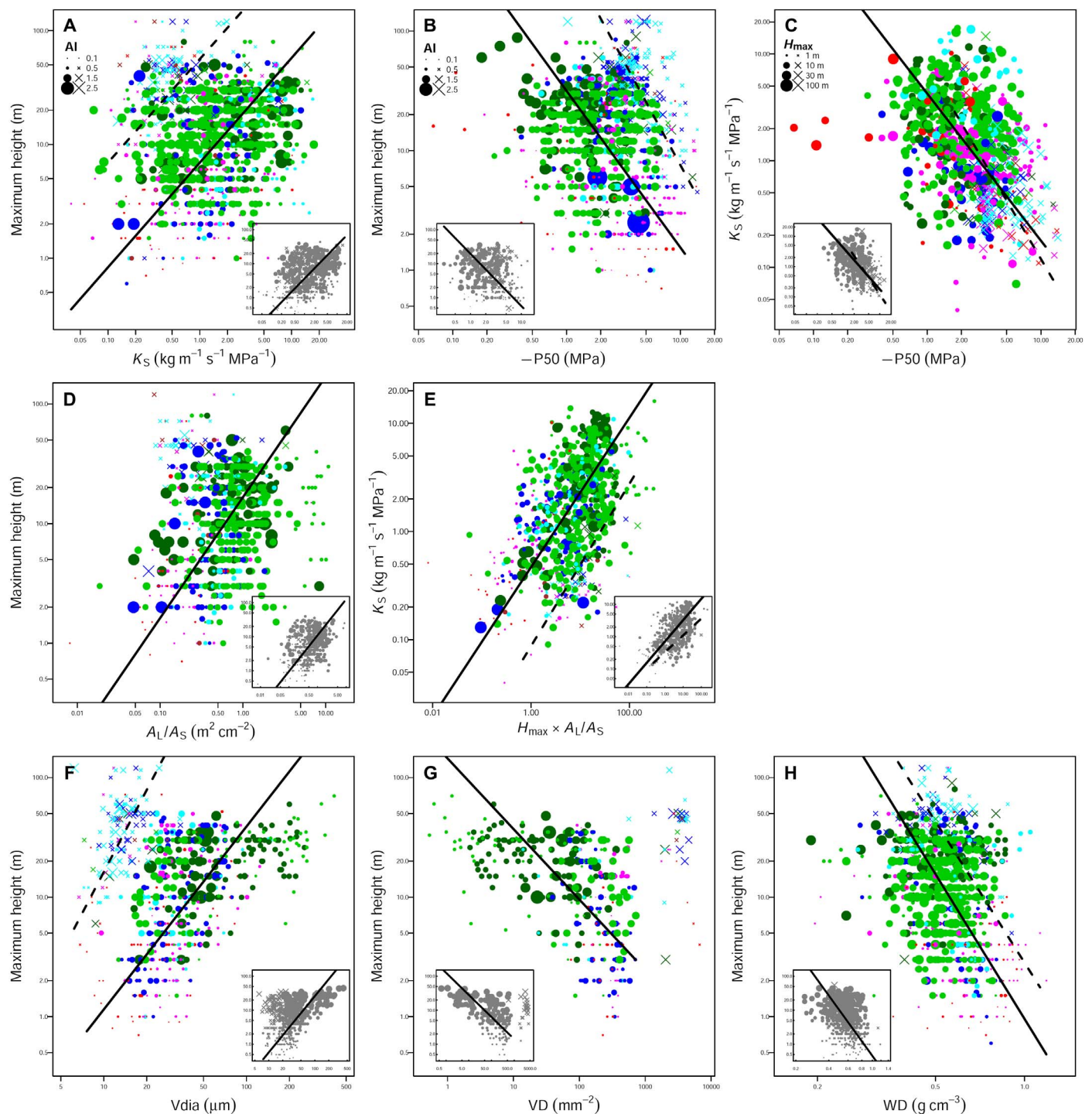


Fig. 2. Plant height is aligned with hydraulic traits. Relationships between maximum plant height (inset: actual measured plant height) and (A) sapwood-specific hydraulic conductivity (K_s), (B) the xylem tension at 50% loss of the maximum hydraulic conductivity ($P50$), (C) trade-off between K_s and $P50$, (D) leaf-to-sapwood area ratio (A_L/A_S), (E) the product of A_L/A_S and K_s (Darcy's law), (F) mean tangential vessel or tracheid diameter ($Vdia$), (G) number of vessels or tracheids per square millimeter (VD), and (H) sapwood density (WD) across species. Scaling slopes in (E) for angiosperms (0.69 and 0.66 based on H_{max} and H_{actv} respectively) and gymnosperms (0.75 and 0.52 based on H_{max} and H_{actv} respectively) are all significantly less than 1 ($P < 0.001$). Different colors indicate biome types (see Table 1), and symbols for angiosperms (circles, solid lines) and gymnosperms (crosses, dashed lines) are scaled to AI values in (A and B) and (D to H), but to H_{max} values in (C). Model parameters are reported in tables S3 to S6.

Table 2. Effects of AI on the coordination between height and hydraulic traits. LMM and LM for log-log-transformed trait relationships within (A) angiosperm and (B) gymnosperm species. For LMM, one hydraulic trait and AI are fixed factors; site and species are random factors. Sampling sizes (*n*), *F* values, *P* values (**P* <0.05, ***P* <0.01, and ****P* <0.001), variance components of random factors and residuals, and *R*² for each model are reported. Models for other traits are reported in table S7.

Model	<i>n</i>	(A) Angiosperm		<i>n</i>	(B) Gymnosperm	
<i>H</i>_{max} ~ <i>K</i>_s × AI	1127	LMM	LM	162	LMM	LM
Fixed effect		<i>F</i> ^P	<i>F</i> ^P		<i>F</i> ^P	<i>F</i> ^P
Trait		57.84***	119.38***		0.48	7.30**
AI		50.98***	132.56***		0.67	0.60**
Trait × AI		5.49*	4.98*		0.27	6.99
Random effect		Variance component			Variance component	
Species	870	0.550		97	0.651	
Site	163	0.066		87	0.000	
Residual		0.059			0.006	
<i>R</i> ² _{fixed}		0.14			0.00	
<i>R</i> ² _{all}		0.92	0.19		0.98	0.09
<i>H</i>_{max} ~ <i>P</i>50 × AI	954	LMM	LM	253	LMM	LM
Fixed effect		<i>F</i> ^P	<i>F</i> ^P		<i>F</i> ^P	<i>F</i> ^P
Trait		13.18***	87.42***		2.15	64.12***
AI		29.40***	138.26***		0.02	0.12
Trait × AI		0.98	11.90***		0.17	7.45**
Random effect		Variance component			Variance component	
Species	684	0.761		131	0.627	
Site	215	0.007		126	0.002	
Residual		0.038			0.003	
<i>R</i> ² _{fixed}		0.04			0.00	
<i>R</i> ² _{all}		0.95	0.20		0.99	0.22
<i>K</i>_s ~ <i>P</i>50 × <i>H</i>_{max}	660	LMM	LM	147	LMM	LM
Fixed effect		<i>F</i> ^P	<i>F</i> ^P		<i>F</i> ^P	<i>F</i> ^P
<i>P</i> 50		7.53*	70.61***		2.71	21.2***
<i>H</i> _{max}		17.4***	28.41***		0.01	2.19
<i>P</i> 50 × <i>H</i> _{max}		0.54	1.28		0.46	2.30
Random effect		Variance component			Variance component	
Species	494	0.395		89	0.150	
Site	130	0.357		82	0.263	
Residual		0.168			0.218	
<i>R</i> ² _{fixed}		0.09			0.18	

continued on next page

Model	n	(A) Angiosperm		n	(B) Gymnosperm	
R^2_{all}		0.83	0.13		0.72	0.13
$H_{max} \sim A_L/A_S \times AI$	739	LMM	LM	74	LMM	LM
Fixed effect		F^P	F^P		F^P	F^P
Trait		25.86***	100.04***		0.00	0.06
AI		5.17**	49.93***		0.00	1.03
Trait \times AI		6.49**	5.80**		0.00	2.40
Random effect		Variance component			Variance component	
Species	637	0.529		43	0.283	
Site	84	0.094		42	0.000	
Residual		0.073			0.000	
R^2_{fixed}		0.17			0.00	
R^2_{all}		0.91	0.17		0.99	0.05
$H_{max} \sim Vdia \times AI$	574	LMM	LM	145	LMM	LM
Fixed effect		F^P	F^P		F^P	F^P
Trait		56.52***	311.62***		0.03	43.13***
AI		11.16**	101.61***		0.12	15.12***
Trait \times AI		4.11*	2.18		0.01	12.42***
Random effect		Variance component			Variance component	
Species	506	0.567		88	0.515	
Site	110	0.084		79	0.000	
Residual		0.011			0.005	
R^2_{fixed}		0.33			0.00	
R^2_{all}		0.99	0.42		0.99	0.33
$H_{max} \sim VD \times AI$	343	LMM	LM	38	LMM	LM
Fixed effect		F^P	F^P		F^P	F^P
Trait		33.73***	147.93***		0.00	0.45
AI		0.00	26.37***		0.00	7.06*
Trait \times AI		0.91	2.58		0.00	10.14**
Random effect		Variance component			Variance component	
Species	320	0.583		33	0.566	
Site	36	0.067		26	0.000	
Residual		0.012			0.000	
R^2_{fixed}		0.26			0.00	
R^2_{all}		0.99	0.34		0.99	0.34

continued on next page

Model	n	(A) Angiosperm		n	(B) Gymnosperm	
$H_{\max} \sim \text{WD} \times \text{AI}$	995	LMM	LM	160	LMM	LM
Fixed effect		F^P	F^P		F^P	F^P
Trait		17.22***	125.36***		0.11	34.63***
AI		53.55***	151.18***		0.12	12.34***
Trait \times AI		8.62**	10.53**		0.02	12.92***
Random effect		Variance component			Variance component	
Species	815	0.510		100	0.531	
Site	118	0.122		79	0.000	
Residual		0.060			0.005	
R^2_{fixed}		0.22			0.00	
R^2_{all}		0.93	0.22		0.99	0.28

and AI, with or without their interaction effects). For the random factors, 60 to 90% of the random variance was explained by species compared with 10 to 20% by site (e.g., for $H_{\max} \sim K_s \times \text{AI}$, the variance components for species and site were 0.550 and 0.066, respectively). In the equivalent LMs, without random effects, hydraulic traits and AI together explained 19 to 42% of the total variation in H_{\max} (Table 2A). For gymnosperms, the same model of the six hydraulic traits with H_{\max} and AI had insignificant factor effects in LMMs and low explanatory power (5 to 34%) in LMs (Table 2B).

Synthesis: Principal components analysis and path analyses

Principal components analysis (PCA) on angiosperms based on five traits showed that PC1 and PC2 explained 45 and 19% of total variation, respectively (Fig. 3, A and B). H_{\max} was closely related to AI, whereas K_s , WD, and P50 formed a nearly orthogonal “hydraulic” axis of variation (Fig. 3A). Species could be distinguished by life form (shrubs versus trees) along this hydraulic axis, with shrubs having higher WD, lower K_s , and more negative P50 (Fig. 3B). Similarly, within gymnosperms, PC1 and PC2 explained 46 and 22% of total variation, respectively (Fig. 3, C and D). AI and P50 formed one key axis of variation, whereas H_{\max} , K_s , and WD formed another axis (Fig. 3C). Only life form could be separated in the PCA plot for both angiosperms and gymnosperms (Fig. 3D). Results for PCA on six traits were very similar, except that the added A_L/A_S occupied a position near H_{\max} for angiosperms and a position near K_s for gymnosperms (fig. S4).

Path analyses revealed similar trait associations as PCA. Considering only angiosperms, AI exhibited a large (i.e., steep standardized slope coefficient) and highly significant effect on H_{\max} , whereas after keeping the effect of AI on H_{\max} constant, the effects of P50 and K_s on H_{\max} were weak, albeit significant (Fig. 4A). This does not mean that covariation between P50 (or K_s) and H_{\max} was not meaningful (see table S2) but rather that covariation between P50 and H_{\max} was also aligned with covariation between AI and H_{\max} , i.e., AI appeared to be a key climate variable aligned with both H_{\max} and hydraulics. In contrast, among gymnosperms, the direct effect of AI on H_{\max} was weak and nonsignificant (as expected from the PCA), whereas the xylem traits K_s and P50 appeared to be more proximally linked to H_{\max} than was AI (Fig. 4B).

DISCUSSION

Our results suggest that taller woody species occur in biomes with higher water availability, have higher xylem hydraulic conductivity, and are more vulnerable to xylem embolism. To compensate for greater height and evaporative demand, K_s increased (but less than proportionately) to the product of H_{\max} and A_L/A_S , similar to that predicted via Darcy’s law. Congruent with these results, taller species also had wider conduits, lower conduit density, and lower wood density. However, although these correlations were relatively consistent among groups (common SMA slopes) of life form, leaf form, and biome (with several biome exceptions), habitat water availability and species often modified the slope and intercept coefficients and thus were also important in explaining variance in plant height. Furthermore, we note that the across-species analysis presented here is, to a large extent, dissimilar from within-species studies that have explored similar relationships between plant height and hydraulic traits (3, 8, 10, 11, 31), suggesting that intrinsic evolutionary differences across species and plastic differences within species may have separate influence on plant height and hydraulic trait associations. This study extends our understanding of hydraulic architecture from local studies to a broader range of taxa and biomes across the globe, highlighting that hydraulic traits and plant height may serve as useful measurements for predicting future distributions of species under climate change scenarios.

Plant height is aligned with the hydraulic safety-efficiency trade-off

Besides the general trade-off between K_s and P50 found in previous studies (18), here we have shown that tall species from wet habitats tend to be located at one end of the $K_s \sim \text{P50}$ axis (exhibiting high K_s and P50), while short species from arid habitats tended to be located at the other end of this axis and exhibited the opposite traits (Fig. 2C), i.e., trees and shrubs shared a common $K_s \sim \text{P50}$ slope (table S5). This result is in contrast to the hypothesis that differences in height would confound and obscure this relationship, i.e., that taller species would exhibit a higher K_s at a given P50 than shorter species. This pattern suggests that height, safety, efficiency, and closely associated hydraulic

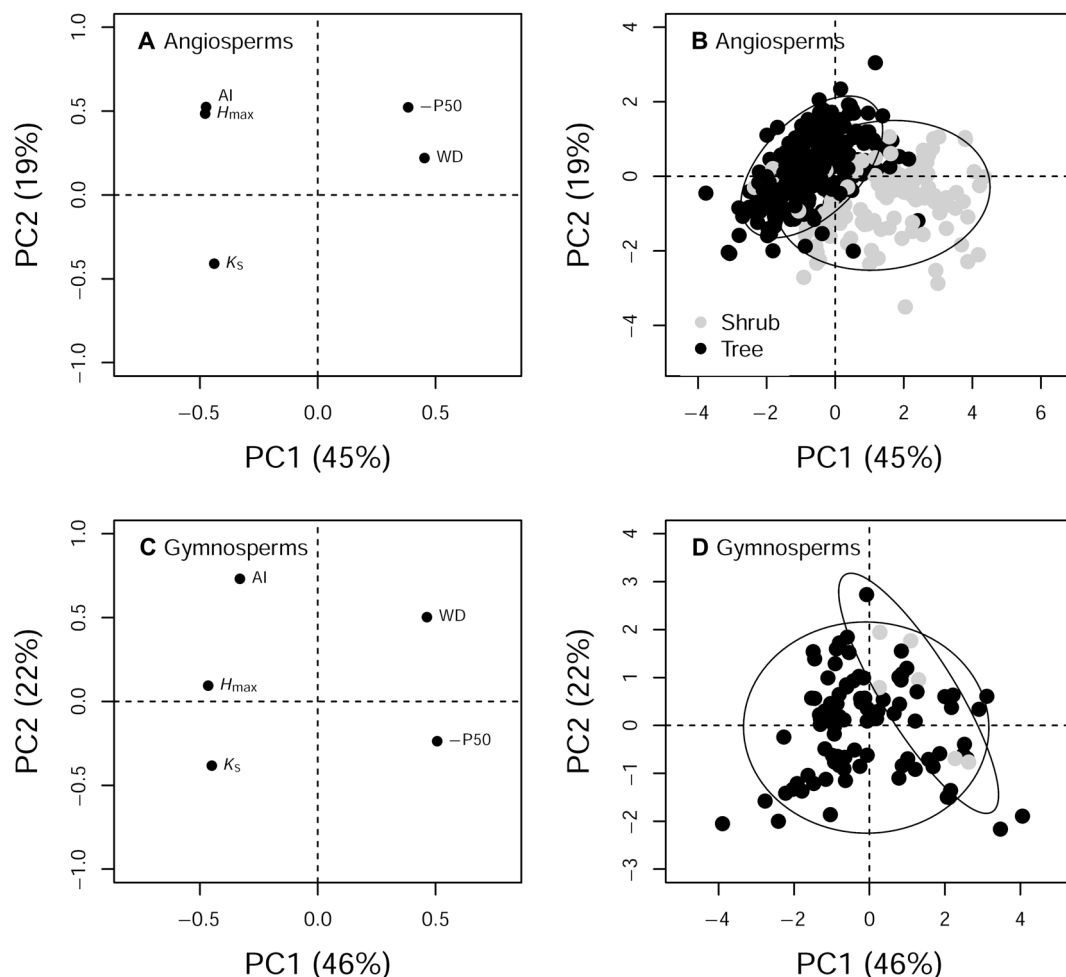


Fig. 3. PCA on plant height, hydraulic traits, and AI. (A and B) Four hundred thirty-one angiosperm species and (C and D) 96 gymnosperm species based on five traits. (A and C) The first two PC loadings and (B and D) species scores with trees (black circles) and shrubs (gray circles) are shown. The percentages of variance explained by the first two PCs are reported in the axis labels. See fig. S4 for PCA on 270 angiosperm and 30 gymnosperm species based on six traits.

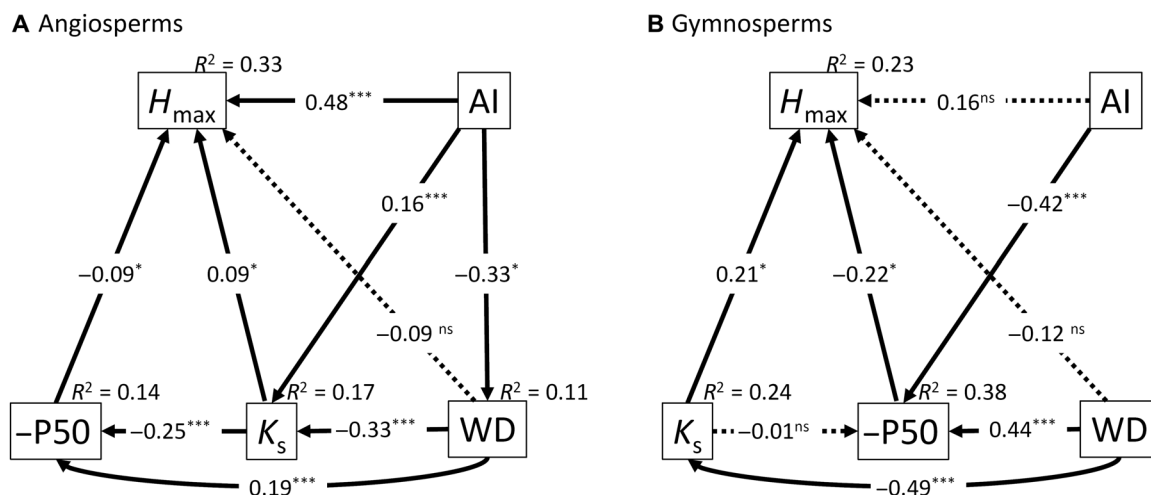


Fig. 4. Path analysis on plant height, hydraulic traits, and AI. (A) Four hundred thirty-one angiosperms ($\chi^2 = 3.63$, $P = 0.06$, standardized root mean square residual (SRMR) = 0.02, normed fit index (NFI) = 0.99) and (B) 96 gymnosperms ($\chi^2 = 2.99$, $P = 0.08$, SRMR = 0.04, NFI = 0.97). Arrows indicate the proposed links between variables. Standardized path coefficients are shown on the arrows [not significant (ns), $P > 0.05$; * $P < 0.05$; *** $P < 0.001$]. Dotted lines indicate nonsignificant paths. R^2 next to the endogenous variables indicate their explained variance.

traits, represent a single weak bundle of traits that are likely important for species sorting processes at the global scale.

Although positive correlation between K_s and P50 was found for all bivariate tests within different groups examined in this study (e.g., biomes and life forms), the path analyses suggested that correlation between K_s and P50 among gymnosperms is not a direct relationship, i.e., it is not likely a “trade-off.” In addition, although K_s and P50 contributed similarly to H_{\max} within angiosperms and gymnosperms, AI exhibited strong and direct linkage with both K_s and WD within angiosperms, whereas AI exhibited direct linkage with only P50 within gymnosperms. This suggests a potential divergence in hydraulic coordination between angiosperms and gymnosperms that we discuss below.

Darcy's law and contrasting height-associated hydraulic strategies within and across species

Our results confirmed that the marked variation in K_s among species was sufficient to offset both increasing height and increasing evaporative demand ($\sim A_L/A_S$) across biomes (21, 22). Hence, A_L/A_S and K_s appeared to be key factors in regulating plant water balance in the face of both habitat aridity and the advantages obtained through greater height. However, these results across species might differ from within species patterns (3, 8, 10, 11, 31).

Within an individual tree, the decreasing of A_L/A_S in taller branches could potentially compensate for hydraulic limitation (10, 24). For example, it has been suggested that xylem embolization may be prevented via leaf area reduction (lower A_L/A_S), in addition to regulation at the stomata (32). In contrast, our across-species data showed that A_L/A_S and leaf area generally increased with increasing height. This is consistent with other empirical studies (18, 22) and hydraulic theory (33). This may indicate that species with sufficient water supply tend to grow taller and maximize their water use and growth (high A_L/A_S) rather than use water more conservatively. It is possible that higher A_L/A_S and H_{\max} may have evolved in taller species because they tend to occupy higher radiation habitats at the top of forest canopies. Therefore, at the global scale, it appears that K_s may be a key trait that has been favored in wet habitats to maintain plant water balance and compensate for increasing height (higher resistance) and A_L/A_S (higher water demand).

Although K_s appeared to be an important across-species trait, in principle, any trait in Darcy's law could compensate for any other trait. For example, longer path length (i.e., greater height) may be associated with increased water limitation (lower xylem water potential) resulting from both friction and gravity. Leaves of higher branches under large negative tension (e.g., low Ψ_{mid}) adjust accordingly to their specific water regime, such as reducing stomatal conductance and maintaining leaf turgor (Ψ_{tlp}) via osmotic adjustment (3). Consequently, the xylem tissue in higher branches might adjust concomitantly (e.g., lower K_s and Ψ_{tlp}) to meet a different water demand and/or maintain a margin of hydraulic safety under the risk of embolism (10). However, in contrast to this theory, our across-species data suggested that taller species tended to occur in wet habitats and had relatively higher Ψ_{mid} , Ψ_{tlp} , and K_s than shorter species. This agrees with an across-species study on Magnoliaceae, which revealed that tall trees had less negative Ψ_{tlp} than shrubs (34) and that higher Ψ_{mid} and Ψ_{tlp} may facilitate faster rates of cell division and expansion, thus increasing the growth of upper canopy species (35). It is also possible that K_s is important for achieving water balance across species (22) because higher K_s should contribute to a smaller water potential gradient between the soil and the terminal organs (thus less negative

Ψ_{mid}) and consequently be related to low levels of embolism in both branches and leaves in wet habitats (less negative P50) (36).

Evidence for increased drought avoidance of tall species comes from two other correlations in our data. First, taller species tended to have less negative Ψ_{pre} , indicating a narrower leaf-to-soil water potential gradient (37), driven in part by a sufficient supply of water delivered via deep roots (38). Second, low wood density, and presumably higher sapwood capacitance, was evident among tall species in this study, as well as from other reports (29, 39), and suggests that tall species may avoid embolization by accessing water stored in sapwood during drought or periods of high demand (28). Stem water storage may also partially compensate for increases in axial hydraulic resistance with tree height and thus take part in regulating the water status of leaves exposed to large diurnal variations in evaporative demand in the upper canopy of some forest ecosystems (40). In addition, strong positive correlation between H_{\max} and Vdia in our data suggests that taller angiosperm species may be more susceptible to embolization due to a greater frequency of large diameter vessels (27).

Coordination between height and hydraulic traits was altered by phylogeny, biome, and life form

Relationships among hydraulic traits and plant height should be an evolutionary outcome of multiple selection pressures acting across and within habitats (2, 41). Several hypotheses addressing the hydraulic limitations imposed by height have been based on phenotypic comparisons within species, and as such, considering phylogeny in these analyses may help to explain when a particular trait correlation evolved, in which clades, and whether trait coordinations have arisen independently more than once. In addition, we might not necessarily expect variation across species and variation within species to result in similar correlations among traits, as has been found for leaf economic traits (42, 43).

In this study, we considered the most contrasting phylogenetic clades, angiosperms, and gymnosperms, which differed markedly in both structural and functional traits. For example, none of the tracheid traits measured for gymnosperms correlated with H_{\max} , except a weak positive correlation between H_{\max} and Vdia. Recent work on gymnosperm hydraulics suggests that the overlap between the torus and margo structures, not the size of the torus or margo themselves, relate to hydraulic safety, whereas the torus-margo overlap may have little to do with hydraulic efficiency (44). Thus, clade-specific conduit and pit ultrastructures are likely to have contributed to differences in efficiency-safety relationships between angiosperms and gymnosperms in this study. Furthermore, although angiosperms occupied a similar climatic range as gymnosperms, angiosperms showed much wider ranges in all traits examined in this study. If this variation is adaptive, then angiosperms may be better suited to diverse habitats. For instance, many angiosperm species can operate at negative hydraulic safety margins (20). It is also likely that the marked departure of H_{\max} from H_{act} among gymnosperms also weakened hydraulic-height relationships (insets in Figs. 1 and 2), possibly confirming that hydraulic traits are linked more strongly with H_{\max} than with H_{act} at least among gymnosperms.

Habitat water availability differed markedly among the biomes considered in this study. There appears to be no strong argument for why relationships between hydraulic traits and plant height should exhibit differences in the fitted slope coefficients. All the significant relationships between H_{\max} and hydraulic traits showed similar trends among biomes. For example, AI strongly affected the coordination between plant height and all the hydraulic traits examined in this study, which almost certainly explain the contradiction between the empirical

correlations reported here (specifically, positive correlation between plant height and A_L/A_S and the balancing effect of K_S), with predictions arising from physiological theories based on single individuals. The key to understanding this apparent contradiction is that soil water increased across habitats, which allowed for higher evaporative loss from the canopy (per unit xylem cross section) and greater path length resistance (arising from height), and also increased K_S and/or increased capacitance (30). Hence, higher K_S appeared to compensate for higher evaporative water loss, as well as greater path length resistance, across species and habitats. It is also possible that factors other than hydraulics may place meaningful limitations on plant height, e.g., biomechanical and energetic limitations (11, 15). These other possible limiting factors might also explain some of the variance in H_{\max} that was not accounted for by hydraulics.

Life form was found as the most distinctive group, but many relationships between H_{\max} and functional traits were only significant within shrubs, and all the significant slopes were steeper in shrubs than in trees. Within angiosperms, H_{\max} increased significantly with increasing AI within shrubs but showed a decreasing trend (although not significant) within trees (table S5). Shorter tree species from temperate and tropical forests, and the tallest tree species mainly distributed in temperate areas (15), were the main drivers of this decreasing pattern. This finding could help to explain the hump-shaped curve between global forest canopy height and water availability found in a recent study, besides its proposed physiological reasons (45). Our dataset confirmed that the height of trees (main canopy component) may exhibit weak and, even sometimes, negative association with water availability (e.g., tropical forests), whereas shrubs were often responsible for the underlying across-biome relationships between H_{\max} and hydraulic traits. Furthermore, differences between shrubs and trees were more evident than between evergreen and deciduous species. One possible reason for this was that most hydraulic traits in this study (all traits involved in the PCA) were branch-based measurements, which may not be aligned with leaf strategies. A more comprehensive combination of traits may better represent the spectrum of plant form and function (2).

MATERIALS AND METHODS

Data collection

Four categories of data were collected:

1) Plant hydraulic traits. We obtained xylem hydraulic efficiency and safety traits for as many species and study sites as possible but avoided herbs, grasses, cacti, and lianas to consider only self-supporting woody life forms. Data were confined to measurements taken on the terminal branches of mature plants. For multiple measures on the same species from the same site, we used mean values. In total, our dataset included 1843 observations—1281 species from 369 sites worldwide with 11 functional traits. Within the 1843 observations, 1267 observations were from the TRY Plant Traits Database (46), 365 observations were collected from recent literature, and 211 observations were measured in this study (full dataset and references are in table S1).

Maximum sapwood-specific hydraulic conductivity (K_S), leaf-specific hydraulic conductivity (K_L), the xylem tension at 50% loss of the maximum hydraulic conductivity (P50), and leaf-to-sapwood area ratio (A_L/A_S) of small, terminal branches (0.4 to 1.0 cm in diameter) were used because these sizes were most commonly reported in literature. Four structural traits that are related with plant hydraulics were also obtained from the terminal branches as well: sapwood density (WD),

mean tangential vessel (angiosperms) or tracheid (gymnosperms) diameter (V_{dia}), vessel or tracheid density (VD), and maximum vessel length (only angiosperms, VL_{\max}). Minimum water potential at pre-dawn (Ψ_{pre}), water potential at midday (Ψ_{mid}), and leaf turgor loss point (Ψ_{tp}) were also collected. We note that Ψ_{pre} should be interpreted with some caution because it varies with species, site, and time of the year but has been used as a proxy for local soil water conditions. We also note that A_L/A_S was measured in terminal branches rather than in whole-plants, which are likely biased by size-dependent effects. Nevertheless, A_L often increases near proportionally with A_S , even within large forest trees (47), and as such, our branch A_L/A_S is likely to reflect real differences in whole-plant water use across species. The measurement methods for each trait can be found from references in table S1.

There are still different views on whether xylem resistance increases proportionately with plant height, as the Ohm's law analogy suggests. It is likely that the path length effect in tall species has been minimized via the narrowing of conduit diameter with increasing height (26). Therefore, it is important that the sampling of xylem conductivity and conduit diameter is measured at some standardized location within each plant, e.g., terminal branches. In addition, considering that hydraulic traits are likely determined by both intrinsic differences across species and differences related to stature and ontogeny, we used both maximum and actual measured plant height (H_{act}) when evaluating the linkages between height and hydraulic traits.

Another consideration is the effect of gravity on hydraulic traits, because markedly tall trees may exhibit differences in foliar traits with increasing height, presumably as an adaptation to the lower water potentials arising from gravity. However, even for a 100-m tree, the gravitational potential is -0.98 MPa, whereas the water potential associated with meaningful loss of xylem conductance is generally less than this, particularly among small statured species in our dataset (see below).

2) Maximum plant height (H_{\max}) and actual measured plant height (H_{act}). We gathered H_{\max} for 1281 species from open source publications [e.g., local floras and wikipedia (<https://en.wikipedia.org/wiki/>)], as well as the published literature (48). However, because plants sampled in the field were usually shorter than their maximum attainable height and it was unknown whether hydraulic traits would be linked stronger with H_{\max} or H_{act} , we also recorded the H_{act} of the plants from which the hydraulic traits were measured.

Although only 897 H_{act} observations were recorded, it enabled comparisons with patterns found for H_{\max} . In our dataset, most species were not very tall. The mean H_{\max} of all 1281 species was 17.8 ± 16.2 m (mean \pm SD), 5.1% of which had $H_{\max} \geq 50$ m. The mean H_{act} of all 897 observations was 9.6 ± 8.7 m, only 1.8% of which had $H_{act} \geq 30$ m. Thus, the effect from gravity was likely negligible, relative to the effect of path length and hydraulic demand from the canopy.

3) Biome type for each site. On the basis of the database of Terrestrial Ecoregions of the World (49), we assigned an ecoregion for each site using the function `extract` in the package `raster` (50) in R (51). This was done to assign biome types using a uniform and objective criterion. To concisely summarize, we further classified the 137 ecoregions into seven biome types according to each site's specific descriptions and previous criteria (20) from arid to wet gradients: DES, WDS (woodland/shrubland), BOR, TMS, TMR, TRS (including subtropical forests and tropical and subtropical savanna), and TRR. We compared this biome classification system with the classic Whittaker Biome Classification system based on mean annual precipitation (MAP)

and mean annual temperature (52). We found that both systems were largely consistent with each other. For sites that differed between classification systems, we assigned ecoregions from Olson *et al.* (49) because this system better reflect the distribution of species and communities more accurately than Whittaker (52), which was derived from gross biophysical features (fig. S5).

4) Aridity index (AI). AI was calculated as the ratio of MAP and PET. We plotted and extracted AI values for each site based on the Global Aridity Index database at a 30-arc sec resolution (www.cgiar-csi.org; Fig. 1) (53). Recent studies that have examined many environmental variables have reported that precipitation of the wettest month was the best predictor for maximum plant height (13), whereas the difference between precipitation and PET was the most important variable associated with forest canopy height (54). Considering that evapotranspiration includes more climatic factors than only precipitation, we used AI (MAP/PET) as a proxy for water availability at each site.

Data analyses

All the continuous indices were natural log-transformed to homogenize variance. If the original values were all negative (e.g., P50), then log-transformed absolute values were used. Considering that H_{\max} was our study focus and H_{\max} was also strongly positively correlated with H_{act} (fig. S1), we put H_{act} as insets for comparisons and only reported detailed model results for H_{\max} .

For question 1, the relationships between H_{\max} and K_s or P50 and between K_s and P50 were tested by SMA analysis. Correlation coefficients were calculated to characterize the overall associations across all species and groups (i.e., between angiosperm and gymnosperm, among biomes, or between life forms and leaf forms), whereas differences among groups were compared by evaluating SMA slopes, intercepts, and their position along a common axis. The null expectation (H_0) was that the slope of the regression (or intercept or group shift) would not deviate significantly among groups. SMA analysis was performed using the *sma* function in the *smatr* package (55) in R.

For questions 2 and 3, we tested the assumption based on Darcy's law that K_s should increase near proportionally to the product of height and A_l/A_s (e.g., $K_s \propto H_{\max} \times A_l/A_s$ or $H_{\text{act}} \times A_l/A_s$). We then tested the relationships between H_{\max} and A_l/A_s and other hydraulic traits using the same methods for question 1.

For question 4, we compared LMMs and LMs to explore whether correlations between H_{\max} and other hydraulic traits were affected by AI. Models were simplified to as few traits as possible (e.g., two traits in paired correlation and three variables in LMM). This was done because missing data markedly decreased sample size in models with greater than three variables. For LMMs, we started from a simple model, " $H_{\max} \sim \text{trait} + \text{AI} + (1|\text{site})$ ", with trait and AI as fixed factors and site as a random factor. We then used stepwise model comparison by adding interactions and random factors, including species, family and genus, plant life form and leaf form, and biome type. Last, we selected " $H_{\max} \sim \text{trait} \times \text{AI} + (1|\text{site}) + (1|\text{species})$ " as the best-fit model because it included all meaningful predictors and had the lowest Akaike information criterion value among all models. LMs were built as " $H_{\max} \sim \text{trait} \times \text{AI}$ " for comparing the explanation power of random factors. We fitted LMMs using the *lmer* function in the *lme4* package (56) in R. Statistical significance of fixed factors was assessed by type III sums of squares and Satterthwaite's approximation of denominator degrees of freedom, whereas random factors were assessed using likelihood ratio tests based on the *lmerTest* package (57)

in R, and then, we reported the R^2 for both fixed factors and the entire model (58).

Last, PCA was used to investigate trait coordination and to explore which traits were the most important in distinguishing differences among groups of species. Because of the inconsistent missing data of different traits, we were limited to using no more than five or six traits in the PCA models. PCA was conducted using the *princomp* function in R. We also applied path analyses to explore the relationships among the five traits used in PCA using the *lavaan* package (59) in R. Model structures were chosen primarily based on well-understood relationships among hydraulic traits and not on trait arrangements giving the best-fit outcomes. All traits were scaled to unit variance and mean of zero before fitting. The model fit was evaluated using the χ^2 statistic and the normed fit index.

SUPPLEMENTARY MATERIALS

Supplementary material for this article is available at <http://advances.sciencemag.org/cgi/content/full/5/2/eaav1332/DC1>

Appendix S1. Supplementary results.

Fig. S1. Relationship between H_{\max} and H_{act} .

Fig. S2. Plant height is aligned with leaf water potentials.

Fig. S3. Plant height is aligned with leaf hydraulic traits.

Fig. S4. PCA on plant height, four hydraulic traits, and AI.

Fig. S5. Distribution of sampling sites across the world's major biomes.

Table S1. Full dataset and data sources in this study, with definitions and descriptions for each index.

Table S2. Correlation coefficients among AI, H_{\max} , and the 11 hydraulic traits.

Table S3. SMA regressions and comparisons between angiosperms and gymnosperms for trait pairs.

Table S4. SMA regressions and multiple comparisons among biomes for trait pairs.

Table S5. SMA regressions and comparisons between life forms for trait pairs.

Table S6. SMA regressions and comparisons between leaf forms for trait pairs.

Table S7. Effects of AI on the coordination between height and other hydraulic traits.

REFERENCES AND NOTES

1. M. Westoby, D. S. Falster, A. T. Moles, P. A. Vesk, I. J. Wright, Plant ecological strategies: Some leading dimensions of variation between species. *Annu. Rev. Ecol. Syst.* **33**, 125–159 (2002).
2. S. Diaz, J. Kattge, J. H. C. Cornelissen, I. J. Wright, S. Lavorel, S. Dray, B. Reu, M. Kleyer, C. Wirth, I. C. Prentice, E. Garnier, G. Bönsch, M. Westoby, H. Poorter, P. B. Reich, A. T. Moles, J. Dickie, A. N. Gillison, A. E. Zanne, J. Chave, S. J. Wright, S. N. Sheremet'ev, H. Jactel, C. Baraloto, B. Cerabolini, S. Pierce, B. Shipley, D. Kirkup, F. Casanoves, J. S. Joswig, A. Günther, V. Falczuk, N. Rüger, M. D. Mahecha, L. D. Gorné, The global spectrum of plant form and function. *Nature* **529**, 167–171 (2016).
3. M. G. Ryan, B. J. Yoder, Hydraulic limits to tree height and tree growth. *Bioscience* **47**, 235–242 (1997).
4. J. A. Savage, S. D. Beecher, L. Clerx, J. T. Gersony, J. Knoblauch, J. M. Losada, K. H. Jensen, M. Knoblauch, N. M. Holbrook, Maintenance of carbohydrate transport in tall trees. *Nat. Plants* **3**, 965–972 (2017).
5. I. J. Wright, P. B. Reich, M. Westoby, D. D. Ackerly, Z. Baruch, F. Bongers, J. Cavender-Bares, T. Chapin, J. H. C. Cornelissen, M. Diemer, J. Flexas, E. Garnier, P. K. Groom, J. Gulias, K. Hikokasa, B. B. Lamont, T. Lee, W. Lee, C. Lusk, J. J. Midgley, M.-L. Navas, Ü. Niinemets, J. Oleksyn, N. Osada, H. Poorter, P. Poot, L. Prior, V. I. Pyankov, C. Roumet, S. C. Thomas, M. G. Tjoelker, E. J. Veneklaas, R. Villar, The worldwide leaf economics spectrum. *Nature* **428**, 821–827 (2004).
6. J. Chave, C. Andalo, S. Brown, M. A. Cairns, J. Q. Chambers, D. Eamus, H. Fölster, F. Fromard, N. Higuchi, T. Kira, J.-P. Lescure, B. W. Nelson, H. Ogawa, H. Puig, B. Riéra, T. Yamakura, Tree allometry and improved estimation of carbon stocks and balance in tropical forests. *Oecologia* **145**, 87–99 (2005).
7. C. O. Marks, H. C. Muller-Landau, D. Tilman, Tree diversity, tree height and environmental harshness in eastern and western North America. *Ecol. Lett.* **19**, 743–751 (2016).
8. J.-C. Domec, B. Lachenbruch, F. C. Meinzer, D. R. Woodruff, J. M. Warren, K. A. McCulloh, Maximum height in a conifer is associated with conflicting requirements for xylem design. *Proc. Natl. Acad. Sci. U.S.A.* **105**, 12069–12074 (2008).
9. T. J. Givnish, On the adaptive significance of leaf height in forest herbs. *Am. Nat.* **120**, 353–381 (1982).

10. G. W. Koch, S. C. Sillett, G. M. Jennings, S. D. Davis, The limits to tree height. *Nature* **428**, 851–854 (2004).
11. T. J. Givnish, S. C. Wong, H. Stuart-Williams, M. Holloway-Phillips, G. D. Farquhar, Determinants of maximum tree height in *Eucalyptus* species along a rainfall gradient in Victoria, Australia. *Ecology* **95**, 2991–3007 (2014).
12. D. S. Falster, M. Westoby, Plant height and evolutionary games. *Trends Ecol. Evol.* **18**, 337–343 (2003).
13. A. T. Moles, D. I. Warton, L. Warman, N. G. Swenson, S. W. Laffan, A. E. Zanne, A. Pitman, F. A. Hemmings, M. R. Leishman, Global patterns in plant height. *J. Ecol.* **97**, 923–932 (2009).
14. M. Rueda, O. Godoy, B. A. Hawkins, Spatial and evolutionary parallelism between shade and drought tolerance explains the distributions of conifers in the conterminous United States. *Global Ecol. Biogeogr.* **26**, 31–42 (2017).
15. M. Larjavaara, The world's tallest trees grow in thermally similar climates. *New Phytol.* **202**, 344–349 (2014).
16. M. E. Olson, D. Soriano, J. A. Rosell, T. Anfodillo, M. J. Donoghue, E. J. Edwards, C. León-Gómez, T. Dawson, J. J. Camarero Martínez, M. Castorena, A. Echeverría, C. I. Espinosa, A. Fajardo, A. Gazol, S. Isnard, R. S. Lima, C. R. Marcati, R. Méndez-Alonso, Plant height and hydraulic vulnerability to drought and cold. *Proc. Natl. Acad. Sci. U.S.A.* **115**, 7551–7556 (2018).
17. B. Schuldt, F. Knutzen, S. Delzon, S. Jansen, H. Müller-Haubold, R. Burtlett, Y. Clough, C. Leuschner, How adaptable is the hydraulic system of European beech in the face of climate change-related precipitation reduction? *New Phytol.* **210**, 443–458 (2016).
18. S. M. Gleason, M. Westoby, S. Jansen, B. Choat, U. G. Hacke, R. B. Pratt, R. Bhaskar, T. J. Brodribb, S. J. Bucci, K.-F. Cao, H. Cochard, S. Delzon, J.-C. Domec, Z.-X. Fan, T. S. Feild, A. L. Jacobsen, D. M. Johnson, F. Lens, H. Maherali, J. Martínez-Vilalta, S. Mayr, K. A. McCulloh, M. Mencuccini, P. J. Mitchell, H. Morris, A. Nardini, J. Pittermann, L. Plavcová, S. G. Schreiber, J. S. Sperry, I. J. Wright, A. E. Zanne, Weak tradeoff between xylem safety and xylem-specific hydraulic efficiency across the world's woody plant species. *New Phytol.* **209**, 123–136 (2016).
19. W. R. L. Anderegg, T. Klein, M. Bartlett, L. Sack, A. F. A. Pellegrini, B. Choat, S. Jansen, Meta-analysis reveals that hydraulic traits explain cross-species patterns of drought-induced tree mortality across the globe. *Proc. Natl. Acad. Sci. U.S.A.* **113**, 5024–5029 (2016).
20. B. Choat, S. Jansen, T. J. Brodribb, H. Cochard, S. Delzon, R. Bhaskar, S. J. Bucci, T. S. Feild, S. M. Gleason, U. G. Hacke, A. L. Jacobsen, F. Lens, H. Maherali, J. Martínez-Vilalta, S. Mayr, M. Mencuccini, P. J. Mitchell, A. Nardini, J. Pittermann, R. B. Pratt, J. S. Sperry, M. Westoby, I. J. Wright, A. E. Zanne, Global convergence in the vulnerability of forests to drought. *Nature* **491**, 752–755 (2012).
21. D. Whitehead, W. R. N. Edwards, P. G. Jarvis, Conducting sapwood area, foliage area, and permeability in mature trees of *Picea sitchensis* and *Pinus contorta*. *Can. J. Forest. Res.* **14**, 940–947 (1984).
22. S. M. Gleason, D. W. Butler, K. Ziemińska, P. Waryszak, M. Westoby, Stem xylem conductivity is key to plant water balance across Australian angiosperm species. *Funct. Ecol.* **26**, 343–352 (2012).
23. F. Sterck, R. Zweifel, Trees maintain a similar conductance per leaf area through integrated responses in growth, allocation, architecture and anatomy. *Tree Physiol.* **36**, 1307–1309 (2016).
24. N. McDowell, H. Barnard, B. Bond, T. Hinckley, R. Hubbard, H. Ishii, B. Köstner, F. Magnani, J. Marshall, F. Meinzer, N. Phillips, M. Ryan, D. Whitehead, The relationship between tree height and leaf area: Sapwood area ratio. *Oecologia* **132**, 12–20 (2002).
25. K. A. McCulloh, J. S. Sperry, F. R. Adler, Water transport in plants obeys Murray's law. *Nature* **421**, 939–942 (2003).
26. G. B. West, J. H. Brown, B. J. Enquist, A general model for the structure and allometry of plant vascular systems. *Nature* **400**, 664–667 (1999).
27. J. Pittermann, J. S. Sperry, Analysis of freeze-thaw embolism in conifers: The interaction between cavitation pressure and tracheid size. *Plant Physiol.* **140**, 374–382 (2006).
28. F. C. Meinzer, D. M. Johnson, B. Lachenbruch, K. A. McCulloh, D. R. Woodruff, Xylem hydraulic safety margins in woody plants: Coordination of stomatal control of xylem tension with hydraulic capacitance. *Funct. Ecol.* **23**, 922–930 (2009).
29. K. A. McCulloh, D. M. Johnson, F. C. Meinzer, D. R. Woodruff, The dynamic pipeline: Hydraulic capacitance and xylem hydraulic safety in four tall conifer species. *Plant Cell Environ.* **37**, 1171–1183 (2014).
30. L. S. Santiago, M. E. De Guzman, C. Baraloto, J. E. Vogenberg, M. Brodie, B. Hérault, C. Fortunel, D. Bonal, Coordination and trade-offs among hydraulic safety, efficiency and drought avoidance traits in Amazonian rainforest canopy tree species. *New Phytol.* **218**, 1015–1024 (2018).
31. S. S. Burgess, J. Pittermann, T. E. Dawson, Hydraulic efficiency and safety of branch xylem increases with height in *Sequoia sempervirens* (D. Don) crowns. *Plant Cell Environ.* **29**, 229–239 (2006).
32. N. Phillips, B. J. Bond, N. G. McDowell, M. G. Ryan, A. Schauer, Leaf area compounds height-related hydraulic costs of water transport in Oregon White Oak trees. *Funct. Ecol.* **17**, 832–840 (2003).
33. T. N. Buckley, D. W. Roberts, How should leaf area, sapwood area and stomatal conductance vary with tree height to maximize growth? *Tree Physiol.* **26**, 145–157 (2006).
34. H. Liu, Q. Xu, P. He, L. S. Santiago, K. Yang, Q. Ye, Strong phylogenetic signals and phylogenetic niche conservatism in ecophysiological traits across divergent lineages of Magnoliaceae. *Sci. Rep.* **5**, 12246 (2015).
35. M. K. Bartlett, C. Scoffoni, L. Sack, The determinants of leaf turgor loss point and prediction of drought tolerance of species and biomes: A global meta-analysis. *Ecol. Lett.* **15**, 393–405 (2012).
36. S. M. Gleason, D. W. Butler, P. Waryszak, Shifts in leaf and stem hydraulic traits across aridity gradients in eastern Australia. *Int. J. Plant Sci.* **174**, 1292–1301 (2013).
37. S. J. Bucci, G. Goldstein, F. C. Meinzer, A. C. Franco, P. Campanello, F. G. Scholz, Mechanisms contributing to seasonal homeostasis of minimum leaf water potential and predawn disequilibrium between soil and plant water potential in Neotropical savanna trees. *Trees* **19**, 296–304 (2005).
38. D. Markewitz, S. Devine, E. A. Davidson, P. Brando, D. C. Nepstad, Soil moisture depletion under simulated drought in the Amazon: Impacts on deep root uptake. *New Phytol.* **187**, 592–607 (2010).
39. L. Poorter, I. McDonald, A. Alarcón, E. Fichtler, J.-C. Licona, M. Peña-Claros, F. Sterck, Z. Villegas, U. Sass-Klaassen, The importance of wood traits and hydraulic conductance for the performance and life history strategies of 42 rainforest tree species. *New Phytol.* **185**, 481–492 (2010).
40. G. Goldstein, J. L. Andrade, F. C. Meinzer, N. M. Holbrook, J. Cavelier, P. Jackson, A. Celis, Stem water storage and diurnal patterns of water use in tropical forest canopy trees. *Plant Cell Environ.* **21**, 397–406 (1998).
41. P. B. Reich, I. J. Wright, J. Cavender-Bares, J. M. Craine, J. Oleksyn, M. Westoby, M. B. Walters, The evolution of plant functional variation: Traits, spectra, and strategies. *Int. J. Plant Sci.* **164**, S143–S164 (2003).
42. J. L. D. Osas, M. Katabuchi, K. Kitajima, S. J. Wright, P. B. Reich, S. A. Van Bael, N. J. B. Kraft, M. J. Samaniego, S. W. Pacala, J. W. Lichstein, Divergent drivers of leaf trait variation within species, among species, and among functional groups. *Proc. Natl. Acad. Sci. U.S.A.* **115**, 5480–5485 (2018).
43. L. D. L. Anderegg, L. T. Berner, G. Badgley, M. L. Sethi, B. E. Law, J. HilleRisLambers, Within-species patterns challenge our understanding of the leaf economics spectrum. *Ecol. Lett.* **21**, 734–744 (2018).
44. P. S. Bouche, M. Larter, J.-C. Domec, R. Burtlett, P. Gasson, S. Jansen, S. Delzon, A broad survey of hydraulic and mechanical safety in the xylem of conifers. *J. Exp. Bot.* **65**, 4419–4431 (2014).
45. S. Tao, Q. Guo, C. Li, Z. Wang, J. Fang, Global patterns and determinants of forest canopy height. *Ecology* **97**, 3265–3270 (2016).
46. J. Kattge, S. Díaz, S. Lavorel, I. C. Prentice, P. Leadley, G. Bönisch, E. Garnier, M. Westoby, P. B. Reich, I. J. Wright, J. H. C. Cornelissen, C. Violle, S. P. Harrison, P. M. Van Bodegom, M. Reichstein, B. J. Enquist, N. A. Soudzilovskaia, D. D. Ackerly, M. Anand, O. Atkin, M. Bahn, T. R. Baker, D. Baldocchi, R. Bekker, C. C. Blanco, B. Blonder, W. J. Bond, R. Bradstock, D. E. Bunker, F. Casanoves, J. Cavender-Bares, J. Q. Chambers, F. S. Chapin III, J. Chave, D. Coomes, W. K. Cornwell, J. M. Craine, B. H. Dobrin, L. Duarte, W. Durka, J. Elser, G. Esser, M. Estiarte, W. F. Fagan, J. Fang, F. Fernández-Méndez, A. Fidelis, B. Finegan, O. Flores, H. Ford, D. Frank, G. T. Freschet, N. M. Fyllas, R. V. Gallagher, W. A. Green, A. G. Gutierrez, T. Hickler, S. I. Higgins, J. G. Hodgson, A. Jalili, S. Jansen, C. A. Joly, A. J. Kerkhoff, D. Kirkup, K. Kitajima, M. Kleyer, S. Klotz, J. M. H. Knops, K. Kramer, I. Kühn, H. Kurokawa, D. Laughlin, T. D. Lee, M. Leishman, F. Lens, T. Lenz, S. L. Lewis, J. Lloyd, J. Llusà, F. Louault, S. Ma, M. D. Mahecha, P. Manning, T. Massad, B. E. Medlyn, J. Messier, A. T. Moles, S. C. Müller, K. Nadrowski, S. Naeem, Ü. Niinemets, S. Nöllert, A. Nüske, R. Ogaya, J. Oleksyn, V. G. Onipchenko, Y. Onoda, J. Ordóñez, G. Overbeck, W. A. Ozinga, S. Patiño, S. Paula, J. G. Pausas, J. Peñuelas, O. L. Phillips, V. Pillar, H. Poorter, L. Poorter, P. Poschlod, A. Prinzing, R. Proulx, A. Rammig, S. Reinsch, B. Reu, L. Sack, B. Salgado-Negret, J. Sardans, S. Shiodera, B. Shipley, A. Siefert, E. Sosinski, J.-F. Soussana, E. Swaine, N. Swenson, K. Thompson, P. Thornton, M. Waldram, E. Weiher, M. White, S. White, S. J. Wright, B. Yguel, S. Zaehle, A. E. Zanne, C. Wirth, TRY—A global database of plant traits. *Glob. Chang. Biol.* **17**, 2905–2935 (2011).
47. R. A. Vertessy, R. G. Benyon, S. K. O'Sullivan, P. R. Gribben, Relationships between stem diameter, sapwood area, leaf area and transpiration in a young mountain ash forest. *Tree Physiol.* **15**, 559–567 (1995).
48. A. T. Moles, D. S. Falster, M. R. Leishman, M. Westoby, Small-seeded species produce more seeds per square metre of canopy per year, but not per individual per lifetime. *J. Ecol.* **92**, 384–396 (2004).
49. D. M. Olson, E. Dinerstein, E. D. Wikramanayake, N. D. Burgess, G. V. N. Powell, E. C. Underwood, J. A. D'Amico, I. Itoua, H. E. Strand, J. C. Morrison, C. J. Loucks, T. F. Allnutt, T. H. Ricketts, Y. Kura, J. F. Lamoreux, W. W. Wettengel, P. Hedao, K. R. Kassem, Terrestrial ecoregions of the world: A new map of life on Earth: A new global map of terrestrial ecoregions provides an innovative tool for conserving biodiversity. *Bioscience* **51**, 933–938 (2001).
50. R. Hijmans, J. van Etten, J. Cheng, M. Sumner, M. Mattiuzzi, J. A. Greenberg, O. P. Lamigueiro, A. Bevan, R. Bivand, L. Busetto, M. Canty, D. Forrest, A. Ghosh, D. Golicer, J. Gray, P. Hiemstra; Institute for Mathematics Applied Geosciences, C. Kamey,

- S. Mosher, J. Nowosad, E. Pebesma, E. B. Racine, B. Rowlingson, A. Shortridge, B. Venables, R. Wueest, raster: Geographic data analysis and modeling. R package ver. 2.1–66 (2013).
51. R Development Core Team, *R: A Language and Environment for Statistical Computing* (R Foundation for Statistical Computing, 2013).
 52. R. H. Whittaker, *Communities and Ecosystems*. (MacMillan, ed. 2, 1975), pp. 385.
 53. A. Trabucco, R. Zomer, *Global Aridity Index (Global-Aridity) And Global Potential Evapo-Transpiration (Global-Pet) Geospatial Database* (CGIAR Consortium for Spatial Information, 2009).
 54. T. Klein, C. Randin, C. Körner, Water availability predicts forest canopy height at the global scale. *Ecol. Lett.* **18**, 1311–1320 (2015).
 55. D. I. Warton, R. A. Duursma, D. S. Falster, S. Taskinen, smatr 3—An R package for estimation and inference about allometric lines. *Methods Ecol. Evol.* **2**, 257–259 (2012).
 56. D. Bates, M. Mächler, B. Bolker, S. Walker, Fitting linear mixed-effects models using lme4. *J. Stat. Softw.* **67**, 1–48 (2015).
 57. A. Kuznetsova, P. B. Brockhoff, R. H. B. Christensen, Package ‘lmerTest’. R package version, 2.0–29 (2015).
 58. S. Nakagawa, H. Schielzeth, A general and simple method for obtaining R^2 from generalized linear mixed-effects models. *Methods Ecol. Evol.* **4**, 133–142 (2013).
 59. Y. Rosseel, Lavaan: An R package for structural equation modeling and more. *J. Stat. Softw.* **48**, 1–36 (2012).

Acknowledgments: We are grateful to the TRY initiative on plant traits (www.try-db.org). The TRY initiative and database is hosted, developed, and maintained by J. Kattge and G. Boenisch (Max Planck Institute for Biogeochemistry, Jena, Germany). TRY is currently supported by DIVERSITAS/Future Earth and the German Centre for Integrative Biodiversity Research (iDiv) Halle-Jena-Leipzig. **Funding:** This work was supported by the National Natural Science Foundation of China (31825005, 31670411, and 31570405), Pearl River S&T Nova Program of Guangzhou (201806010083), State Scholarship Fund of China Scholarship Council (201804910141), and the CAS/SAFEA International Partnership Program for Creative Research Teams. **Competing interests:** The authors declare that they have no competing interests. **Author contributions:** H.L. and Q.Y. designed the study. H.L. and S.M.G. performed all the analyses. H.L., S.M.G., G.H., L.H., P.H., and G.G. collected data or provided their field data. H.L. wrote the first draft of the manuscript and all authors contributed substantially to revisions. **Data and materials availability:** All data used in this study are present in table S1.

Submitted 19 August 2018

Accepted 4 January 2019

Published 13 February 2019

10.1126/sciadv.aav1332

Citation: H. Liu, S. M. Gleason, G. Hao, L. Hua, P. He, G. Goldstein, Q. Ye, Hydraulic traits are coordinated with maximum plant height at the global scale. *Sci. Adv.* **5**, eaav1332 (2019).

Hydraulic traits are coordinated with maximum plant height at the global scale

Hui Liu, Sean M. Gleason, Guangyou Hao, Lei Hua, Pengcheng He, Guillermo Goldstein and Qing Ye

Sci Adv **5** (2), eaav1332.

DOI: 10.1126/sciadv.aav1332

ARTICLE TOOLS

<http://advances.sciencemag.org/content/5/2/eaav1332>

SUPPLEMENTARY MATERIALS

<http://advances.sciencemag.org/content/suppl/2019/02/11/5.2.eaav1332.DC1>

REFERENCES

This article cites 54 articles, 5 of which you can access for free
<http://advances.sciencemag.org/content/5/2/eaav1332#BIBL>

PERMISSIONS

<http://www.sciencemag.org/help/reprints-and-permissions>

Use of this article is subject to the [Terms of Service](#)

Science Advances (ISSN 2375-2548) is published by the American Association for the Advancement of Science, 1200 New York Avenue NW, Washington, DC 20005. The title *Science Advances* is a registered trademark of AAAS.

Copyright © 2019 The Authors, some rights reserved; exclusive licensee American Association for the Advancement of Science. No claim to original U.S. Government Works. Distributed under a Creative Commons Attribution NonCommercial License 4.0 (CC BY-NC).